

Schottky barrier inhomogeneity for graphene/Si-nanowire arrays/n-type Si Schottky diodes

Jian-Jhou Zeng (曾建洲) and Yow-Jon Lin (林祐仲)^{a)}

Institute of Photonics, National Changhua University of Education, Changhua 500, Taiwan

(Received 4 February 2014; accepted 21 March 2014; published online 2 April 2014)

The current–voltage characteristics of graphene/Si-nanowire (SiNW) arrays/n-type Si Schottky diodes with and without H₂O₂ treatment were measured in the temperature range of $-150 \sim 150^\circ\text{C}$. The forward-bias current-voltage characteristics were analyzed on the basis of thermionic emission theory. It is found that the barrier height decreases and the ideality factor increases with the decreased temperatures. Such behavior is attributed to barrier inhomogeneities. It is shown that both Schottky barrier inhomogeneity and the T_0 effect are affected by H₂O₂ treatment, implying that charge traps in the SiNWs have a noticeable effect on Schottky barrier inhomogeneity for graphene/SiNWs/n-type Si diodes. © 2014 AIP Publishing LLC. [<http://dx.doi.org/10.1063/1.4870258>]

Graphene is a zero-gap semiconductor and has a very large intrinsic carrier mobility, which makes it a very promising material for incorporation into devices ranging from diodes to transistors.^{1–9} Due to the technological importance of Schottky diodes which are among the most simple of the graphene-Si contact devices, a full understanding of the nature of their electrical characteristics is of great interest. It has been suggested that charge puddles may be responsible for the presence of inhomogeneous Schottky barrier height ($q\phi_B$) in the graphene/Si devices, whose property still remains not fully understood.⁹ In this letter, we report the electrical properties of graphene Schottky contact on the silicon nanowire (SiNW) arrays with and without H₂O₂ treatment. In recent years, solar cells, Schottky diodes, and memory devices based on the SiNWs have attracted great interest.^{10–16} However, due to the large surface-to-volume ratio, SiNWs have a high surface recombination rate.^{17,18} SiNW surface passivation is an even more challenging task due to their small size. A simple technique (that is, H₂O₂ treatment) to find the inhomogeneous $q\phi_B$ for graphene/SiNWs/n-type Si (n-Si) Schottky diodes was developed in this study. Correlation effects were evaluated using the well-known expression for the thermionic emission (TE).^{8,12,15,19} By analyzing these experimental results, we shall discuss on the possible sources of Schottky barrier inhomogeneity.

Four-inch n-Si (100) wafers with resistivity in the range of $1\text{--}10\ \Omega\ \text{cm}$ purchased from Woodruff Tech Company were used in the experiment. The n-Si film thickness was about $525\ \mu\text{m}$. The SiNWs are made by an electroless wet-chemical etching method.^{12,18} The fabrication process of the SiNWs arrays is shown in Ref. 12. The length of SiNWs, as estimated from field emission scanning electron microscopy (SEM), was $535 \pm 5\ \text{nm}$. Cross-sectional and plane SEM images of the SiNWs are shown in Fig. 1 of Ref. 12. Then, some of the SiNWs/n-Si samples were dipped in the H₂O₂ solution at 60°C for 5 min (referred to as H₂O₂-treated SiNWs/n-Si samples), respectively. The graphene sheet was grown by chemical vapor deposition (CVD). The CVD growth

process of the graphene sheet and techniques to transfer graphene onto SiNWs/n-Si substrates are shown in Ref. 20. The graphene/SiNWs/n-Si samples with and without H₂O₂ treatment were then dried at 50°C for 30 min in air. The graphene area is $0.25\ \text{cm}^2$. In ohmic contacts were deposited onto the back surface of n-Si by a sputter coater. The current–voltage (I – V) curves were measured using a Keithley Model-4200-SCS semiconductor characterization system. The I – V characteristics of the devices were measured in the temperature range of $100\text{--}500\ \text{K}$ using a temperature controlled cryostat, which enables us to make measurements in the temperature range from -150 to 150°C by steps of 30°C . The structural property of graphene was examined using Raman spectroscopy. A 532-nm laser was used for excitation. To discuss on the possible sources of Schottky barrier inhomogeneity, the Si 2p core levels of the SiNWs/n-Si surfaces with and without H₂O₂ treatment were analyzed using X-ray photoelectron spectroscopy (XPS).

Figure 1 shows the Raman spectra of the graphene/Cu and graphene/SiNWs/n-Si samples, respectively. Graphene displays a band at $\sim 1345\ \text{cm}^{-1}$, a band at $\sim 1580\ \text{cm}^{-1}$, and

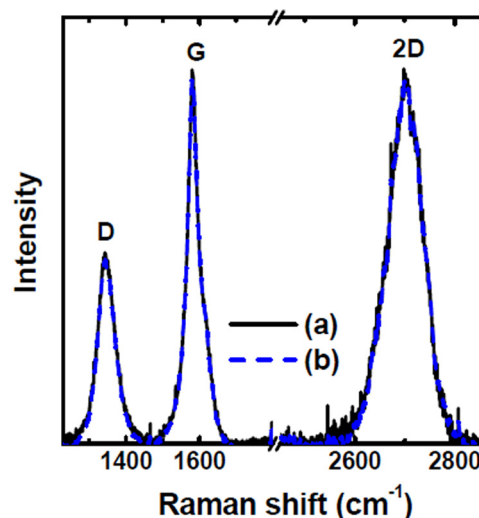


FIG. 1. Raman spectra of (a) graphene/Cu and (b) graphene/SiNWs/n-Si samples.

^{a)}E-mail: rzz2390@yahoo.com.tw. Tel.: 886-4-7232105 ext. 3379. Fax: 886-4-7211153.

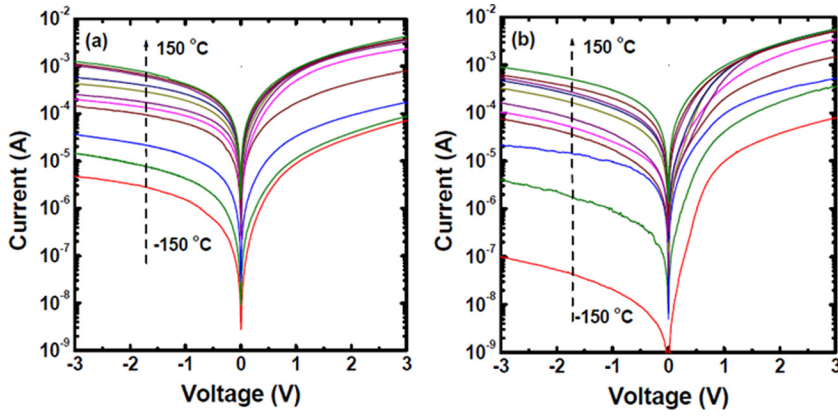


FIG. 2. Temperature-dependent I–V curves of (a) graphene/SiNWs/n-Si and (b) graphene/H₂O₂-treated SiNWs/n-Si Schottky diodes.

a band at $\sim 2700 \text{ cm}^{-1}$ corresponding to the well-documented D, G, and 2D bands.^{4,7,21,22} The amount of disorder in graphene is often correlated with the intensity of the D band.⁴ The G band is assigned to the E_{2g} mode of the relative motion of sp^2 carbon atoms. The intensity of the 2D band is related to the layer numbers of graphene.^{21,22} The ratio of the 2D to G peak intensities was calculated to be close to 1, suggesting that four layers of graphene formed.^{21,22} There were no observable changes in the Raman spectra, implying that techniques to transfer graphene onto SiNWs/n-Si substrates did not induce disorder in graphene.

Figure 2 shows the temperature-dependent I–V characteristics of the graphene/SiNWs/n-Si and graphene/H₂O₂-treated SiNWs/n-Si Schottky diodes, respectively. The rectifying I–V characteristics suggest that Schottky junctions are formed at the graphene/SiNW interfaces. The processing steps used to transfer the CVD-grown graphene typically result in p-doped material with the higher work function than 4.6 eV.^{8,20} The schematic diagram of the band alignment is shown in Fig. 3(a). From TE theory, the I–V characteristic of a Schottky diode is given by^{8,12,15,19}

$$I = I_s \left[\exp\left(\frac{qV}{\eta kT}\right) - 1 \right] = SA^*T^2 \exp\left(-\frac{q\phi_B}{kT}\right) \left[\exp\left(\frac{qV}{\eta kT}\right) - 1 \right], \quad (1)$$

where S is the Schottky contact area, η is the ideality factor, q is the electron charge, T is the absolute temperature, k is the Boltzmann constant, and A^* is the effective Richardson constant ($114 \text{ A cm}^{-2}\text{K}^{-2}$ for n-Si).¹⁹ η is determined from the slope of the linear region of the forward bias $\ln(I)$ – V characteristics. From the curve fitting of I–V characteristic, η and $q\phi_B$ were extracted. Due to the absence of reliable value for the SiNW fill factor, the extracted barrier height can only serve as an approximation.

Figure 3(b) shows η ($q\phi_B$) as a function of temperature. In agreement with the previously reported results for graphene/n-Si Schottky diodes,^{3,6,7,23} we found that the extracted room-temperature $q\phi_B$ values were varied in the range of 0.6–0.7 eV. $\eta > 2$ is found at different temperatures, suggesting that defects at the interface may play important roles in the conduction process. However, H₂O₂ treatment may lead to reduced η and increased $q\phi_B$. It is shown that

$q\phi_B$ decreases and η increases with the decrease in temperatures. According to the Tung's model,²⁴ both η of more than 1 and its linearity vs. $1000/T$ can be convincing evidence of an inhomogeneous $q\phi_B$. In addition, the variation in η with temperature is called the T_0 effect.²⁵ Figure 3(c) shows η as a function of $1000/T$ and the linear fitting curve. Such behaviors of the diode ideality factor have been attributed to particular distribution of states at the SiNW surface.²⁶ η of the diodes showing this behavior varies with temperature as: $\eta = \eta_0 + (T_0/T)$.²⁵ The η_0 and T_0 of graphene/SiNWs/n-Si (graphene/H₂O₂-treated SiNWs/n-Si) Schottky diodes are constants which were found to be 4.23 (3.93) and 940.5 (778.3) K, respectively. H₂O₂ treatment led to reductions in η_0 and T_0 . Explanations of the possible origin of such case may be proposed taking into account the partial energy barrier lowering caused by trapped electrons jumping between the continuous potential well.

Figure 4 shows the conventional Richardson plot of $\ln(I_s/T^2)$ versus T^{-1} and the modified Richardson plot of $\ln(I_s/T^2)$ versus $(\eta T)^{-1}$. As shown in Fig. 4, $\ln(I_s/T^2)$ versus $(\eta T)^{-1}$ is more linear than $\ln(I_s/T^2)$ versus T^{-1} plot for the graphene/SiNWs/n-Si Schottky diode in temperature range measured. Bowing of the experimental $\ln(I_s/T^2)$ versus T^{-1}

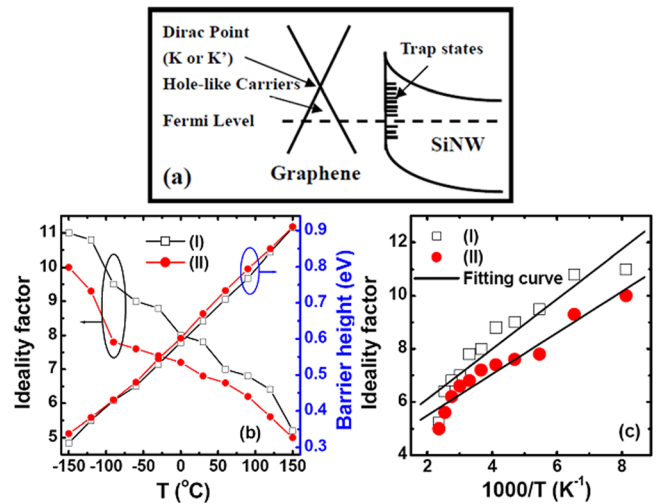


FIG. 3. (a) Energy band diagram of graphene/SiNW heterojunctions, (b) η ($q\phi_B$) as a function of temperature, and (c) η as a function of $1000/T$ [(I) graphene/SiNWs/n-Si and (II) graphene/H₂O₂-treated SiNWs/n-Si Schottky diodes].

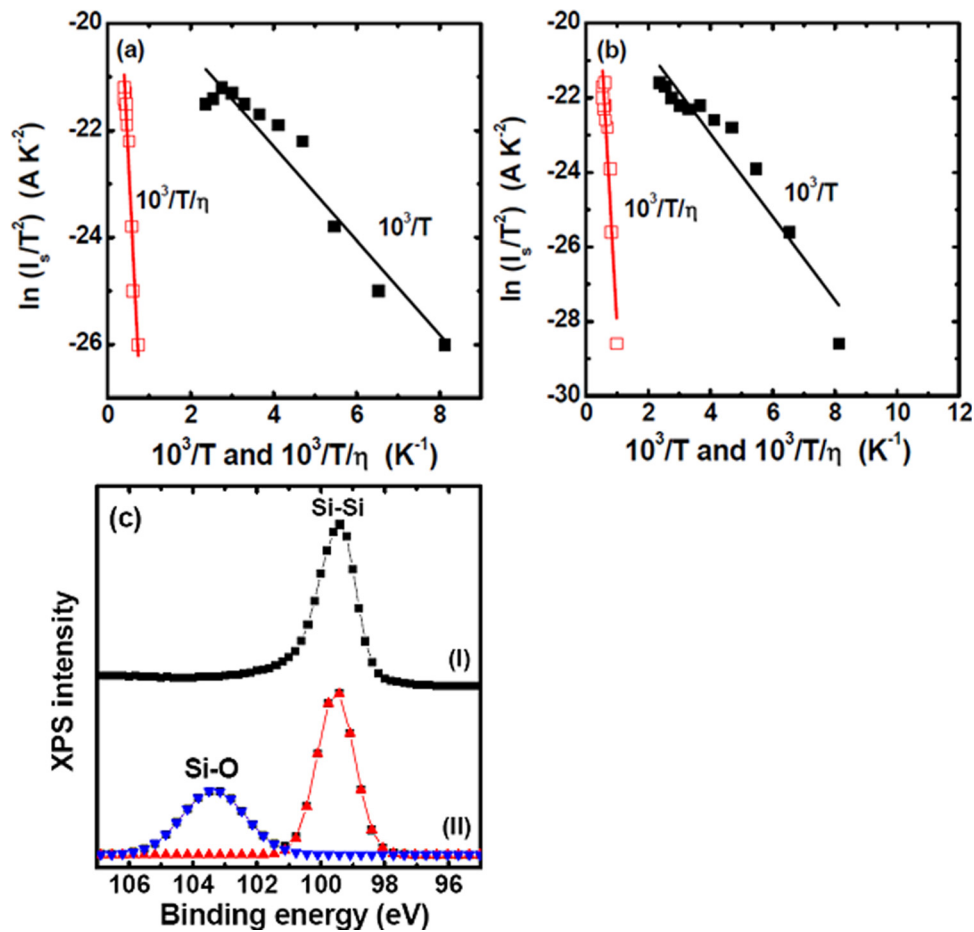


FIG. 4. Richardson plots of $\ln(I_s/T^2)$ versus $10^3(\eta T)^{-1}$ and $\ln(I_s/T^2)$ versus $10^3/T$ [(a) graphene/SiNWs/n-Si and (b) graphene/H₂O₂-treated SiNWs/n-Si Schottky diodes] and (c) Si 2p core-level spectra at the SiNW surfaces (I) without and (II) with H₂O₂ treatment.

curve may be caused by the temperature dependence of $q\phi_B$ due to the existence of the SiNW surface inhomogeneities. To confirm the validity of the TE theory, we calculated the modified Richardson plots of $\ln(I_s/T^2)$ versus $(\eta T)^{-1}$. The calculated values for modified Richardson constants are $1.4 \times 10^{-6} \text{ A cm}^{-2} \text{ K}^{-2}$ for graphene/SiNWs/n-Si Schottky diodes and $2.2 \times 10^{-6} \text{ A cm}^{-2} \text{ K}^{-2}$ for graphene/H₂O₂-treated SiNWs/n-Si Schottky diodes, which are not consistent with the theoretical value of $114 \text{ A cm}^{-2} \text{ K}^{-2}$. The deviation may be due to the spatially inhomogeneous barriers and potential fluctuations at the interface that consist of low and high barrier areas, that is, the current through the diode will

flow preferentially through the lower barriers in the potential distribution.²⁶

Figure 4(c) shows the Si 2p core-level spectra at the SiNW surfaces with and without H₂O₂ treatment, respectively. The peak positioned at ~99.4 eV is attributed to Si-Si bonds and the peak positioned at ~103 eV is attributed to Si-O bonds.¹² It is found the SiNW/n-Si sample with no Si-O peak and the H₂O₂-treated SiNW/n-Si sample with strong Si-O peak. An explanation to the origin of graphene-SiNW interface state is provided by the dangling bonds at the SiNW surfaces. The presence of Si-O bonds might have an effect on the Schottky barrier by reducing the interface state

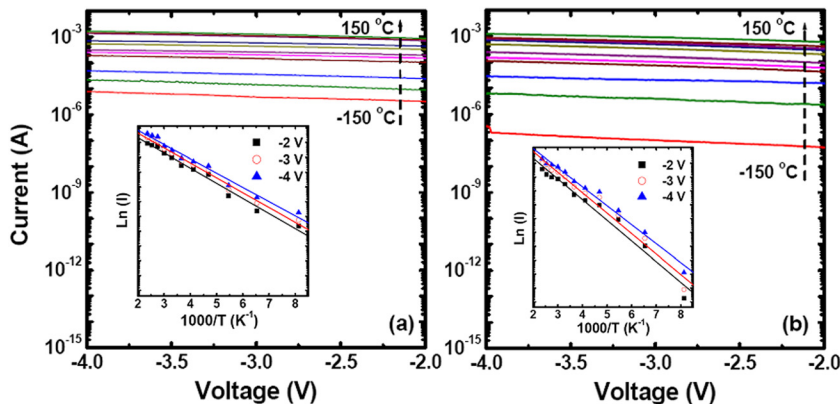


FIG. 5. The reverse-bias log (I)-V curves as a function of temperature [(a) graphene/SiNWs/n-Si and (b) graphene/H₂O₂-treated SiNWs/n-Si Schottky diodes]. Insets: plots of $\ln(I)$ versus $1000/T$ at $V = -2, -3$, and -4 V.

density, indicating that a good passivation is formed at the interface as a result of the reduction of the interfacial defect density and an appropriate interfacial SiO_x layer plays an important role in the conduction process of a Schottky diode.¹² Zhang *et al.* suggested that the Si surface termination state plays key role on the electrical output of the Si-based devices.²⁷ Note, thin SiO_x layer grown by H_2O_2 treatment could be utilized to suppress the recombination velocity.²⁸ In addition, Cho *et al.* found that SiNW surface passivation may lead to the reduced number of charge traps in the SiNWs.¹² As compared to a graphene/SiNWs/n-Si Schottky diode, the number of charge traps in the SiNW near the graphene/SiNW interface is significantly decreased for graphene/ H_2O_2 -treated SiNWs/n-Si Schottky diodes. Consequently, SiNW surface passivation reduced the number of charge traps, causing $\eta_0(T_0)$ to decrease. In this report, we focused on the effects of the dangling bonds at the SiNW surface and suggested that it can be changed by the Si-O bonding. We believe that the inhomogeneous $q\phi_B$ has a strong relation to the reduced number of charge traps on the SiNWs/n-Si sample; and, such result can be attributed to the Si-O bonding. Trap states in the SiNWs near the graphene/SiNW interfaces were considered to affect interfacial barriers with contacts and consequently electrical leakage. We consider to the partial energy barrier lowering caused by trapped electrons jumping between the continuous potential well. The current will flow preferentially through the lower barriers in the potential distribution (that is, electrons hopping from one trap state to another trap state).

To extract the flowed current through the lower barriers (that is, the leakage current), one can measure the reverse-bias I-V characteristics of the devices. In the reverse-bias region, the leakage current is dominant. To determine whether the hopping conduction dominates the reverse-bias conduction behavior, analysis was conducted according to the log (I)-V relationship.²⁹ Figure 5 shows the reverse-bias current of the graphene/SiNWs/n-Si (graphene/ H_2O_2 -treated SiNWs/n-Si) device measured within a temperature range from -150 to 150°C . The leakage current is affected by H_2O_2 treatment. The linear log (I)-V curve is found and the conduction current increases with increasing temperature, indicating that the reverse-bias current exhibits the hopping conduction behavior. The hopping conduction can be expressed as²⁹

$$I = Sq a_m n_e v_f \left[\exp \left(\frac{q a_m V}{2 d k T} - \frac{q \phi_t}{k T} \right) \right], \quad (2)$$

where a_m is the mean hopping distance, n_e is the density of space charge, v_f is the intrinsic vibration frequency, d is the film thickness, and $q\phi_t$ is the barrier height of hopping. The slope (S_L) was extracted from Arrhenius plots at -2 , -3 , and -4 V (the inset of Fig. 5), respectively. Then, we can draw the curve [$S_L = \frac{1}{1000} \left(\frac{q a_m V}{2 d k} - \frac{q \phi_t}{k} \right)$] with a vertical axis of S_L and a lateral axis of V. The $q\phi_t$ extracted from the S_L -V curve is about 94 (141) meV for graphene/SiNWs/n-Si (graphene/ H_2O_2 -treated SiNWs/n-Si) devices. Clearly, $q\phi_t$ is affected by H_2O_2 treatment.

In summary, the origin of Schottky barrier inhomogeneity in the graphene/SiNWs/n-Si Schottky diode was investigated. From the TE theory, H_2O_2 treatment induces the

different linearity of η versus $1000/T$, which can be convincing evidence of an inhomogeneous Schottky barrier. Our experimental results show that both Schottky barrier inhomogeneity and the T_0 effect are affected by H_2O_2 treatment, implying that charge traps in the SiNWs have a noticeable effect on Schottky barrier inhomogeneity for graphene/SiNWs/n-Si diodes. The fitting data of the temperature-dependent I-V curves in the reverse-bias region demonstrated that the corresponding mechanism is related to the hopping conduction. The partial energy barrier lowering caused by trapped electrons jumping between the continuous potential well may lead to the inhomogeneous $q\phi_B$.

The authors acknowledge the support of the Ministry of Science and Technology of Taiwan (Contract No. 100-2112-M-018-003-MY3) in the form of grants.

¹S. D. Sarma, S. Adam, E. H. Hwang, and E. Rossi, *Rev. Mod. Phys.* **83**, 407 (2011).

²A. H. Castro Neto, F. Guinea, N. M. R. Peres, K. S. Novoselov, and A. K. Geim, *Rev. Mod. Phys.* **81**, 109 (2009).

³S. Tongay, T. Schumann, X. Miao, B. R. Appleton, and A. F. Hebard, *Carbon* **49**, 2033 (2011).

⁴S. Tongay, M. Lemaiyre, X. Miao, B. Gila, B. R. Appleton, and A. F. Hebard, *Phys. Rev. X* **2**, 011002 (2012).

⁵D. Dragoman, M. Dragoman, and R. Plana, *J. Appl. Phys.* **108**, 084316 (2010).

⁶C. C. Chen, M. Aykol, C. C. Chang, A. F. J. Levi, and S. B. Cronin, *Nano Lett.* **11**, 1863 (2011).

⁷M. Mohammed, Z. Li, J. Cui, and T. Chen, *Nanoscale Res. Lett.* **7**, 302 (2012).

⁸J. H. Lin, J. J. Zeng, and Y. J. Lin, *Thin Solid Films* **550**, 582 (2014).

⁹C. Yim, N. McEvoy, and G. S. Duesberg, *Appl. Phys. Lett.* **103**, 193106 (2013).

¹⁰X. Wang, K. Q. Peng, X. J. Pan, X. Chen, Y. Yang, L. Li, X. M. Meng, W. J. Zhang, and S. T. Lee, *Angew. Chem., Int. Ed.* **50**, 9861 (2011).

¹¹E. Garnett and P. Yang, *Nano Lett.* **10**, 1082 (2010).

¹²W. M. Cho, Y. J. Lin, H. C. Chang, and Y. H. Chen, *Microelectron. Eng.* **108**, 24 (2013).

¹³W. Lu, Q. Chen, B. Wang, and L. Chen, *Appl. Phys. Lett.* **100**, 023112 (2012).

¹⁴L. He, C. Jiang, H. Wang, D. Lai, Y. H. Tan, C. S. Tan, and Rusli, *Appl. Phys. Lett.* **100**, 103104 (2012).

¹⁵C. H. Ruan and Y. J. Lin, *J. Appl. Phys.* **114**, 143710 (2013).

¹⁶H. Y. Tsao and Y. J. Lin, *Appl. Phys. Lett.* **104**, 053501 (2014).

¹⁷Y. Dan, K. Seo, K. Takei, J. H. Meza, A. Javey, and K. B. Crozier, *Nano Lett.* **11**, 2527 (2011).

¹⁸H. Li, R. Jia, C. Chen, Z. Xing, W. Ding, Y. Meng, D. Wu, X. Liu, and T. Ye, *Appl. Phys. Lett.* **98**, 151116 (2011).

¹⁹Y. J. Lin, B. C. Huang, Y. C. Lien, C. T. Lee, C. L. Tsai, and H. C. Chang, *J. Phys. D: Appl. Phys.* **42**, 165104 (2009).

²⁰Y. J. Lin and J. J. Zeng, *Appl. Phys. Lett.* **102**, 183120 (2013).

²¹Q. Yu, J. Lian, S. Siriponglert, H. Li, Y. P. Chen, and S. S. Pei, *Appl. Phys. Lett.* **93**, 113103 (2008).

²²S. J. Chae, F. Güneş, K. K. Kim, E. S. Kim, G. H. Han, S. M. Kim, H. J. Shin, S. M. Yoon, J. Y. Choi, M. H. Park, C. W. Yang, D. Pribat, and Y. H. Lee, *Adv. Mater.* **21**, 2328 (2009).

²³X. Li, H. Zhu, K. Wang, A. Cao, J. Wei, C. Li, Y. Jia, Z. Li, X. Li, and D. Wu, *Adv. Mater.* **22**, 2743 (2010).

²⁴R. T. Tung, *Phys. Rev. B* **45**, 13509 (1992).

²⁵S. Karatas and S. Altdal, *Mater. Sci. Eng., B* **122**, 133 (2005).

²⁶S. Zhu, R. L. Van Meirhaeghe, C. Detavernier, F. Cardon, G. P. Ru, X. P. Qu, and B. Z. Li, *Solid State Electron.* **44**, 663 (2000).

²⁷F. Zhang, D. Liu, Y. Zhang, H. Wei, T. Song, and B. Sun, *ACS Appl. Mater. Interfaces* **5**, 4678 (2013).

²⁸M. Green, *Sol. Energy* **76**, 3 (2004).

²⁹K. C. Chang, T. M. Tsai, R. Zhang, T. C. Chang, K. H. Chen, J. H. Chen, T. F. Young, J. C. Lou, T. J. Chu, C. C. Shih, J. H. Pan, Y. T. Su, Y. E. Syu, C. W. Tung, M. C. Chen, J. J. Wu, Y. Hu, and S. M. Sze, *Appl. Phys. Lett.* **103**, 083509 (2013).